Research in Astronomy and Astrophysics, 25:075008 (9pp), 2025 July
https://doi.org/10.1088/1674-4527/add8fa
CSTR: 32081.14.RAA.add8fa

NWA 16813 (CK6) Records Almost Highest Oxygen Fugacity in Meteorites

Lei Jin[1,2], Tsz Wai Lo[3], and Ian Tong Fong[3]
[1] State Key Laboratory of Lunar and Planetary Sciences, Macau University of Science and Technology, Macau 999078, China; ljin@must.edu.mo
[2] CNSA Macau Center for Space Exploration and Science, Macau 999078, China
[3] Premier School Affiliated to Hou Kong Middle School, Macau 999078, China
Received 2025 April 20; revised 2025 May 7; accepted 2025 May 12; published 2025 June 26

Abstract

Magnetite-ilmenite pairs in meteorites serve as reliable thermometers and oxygen fugacity (fO_2) indicators for constraining both nebular conditions and thermal metamorphic histories. While CK and CV chondrites exhibit nearly identical petrological characteristics and oxygen isotope compositions, our analysis of NWA 16813 reveals it records the highest fO_2($\log fO_2 = -20.51$ (589.34°C) − $\log fO_2 = -14.21$ (608.63°C)) yet measured among these meteorites. This finding provides critical evidence that CK and CV chondrites experienced fundamentally different redox conditions during their formation. The fO_2 data from NWA 16813, combined with its distinct petrological and mineralogical features, strongly suggest that CK and CV chondrites originated from chemically separate reservoirs in the protoplanetary disk despite their apparent similarities.

Key words: meteorites, meteors, meteoroids – Planetary Systems – minor planets, asteroids: general

1. Introduction

Despite the growing availability of extraterrestrial returned samples, meteorites continue to serve as crucial materials for investigating both nebular and planetary processes. The accurate classification of meteorites constitutes a fundamental yet challenging task in meteoritical research. Among these, carbonaceous chondrites hold particular significance for deciphering the early evolution of the solar system. However, the classification relationship between CV and CK chondrites remains controversial, as they exhibit remarkably similar petrographic characteristics, overlapping oxygen isotopic compositions, comparable cosmic-ray exposure age distributions, and consistent reflectance spectral features—despite having undergone distinctly different thermal histories (Righter & Neff 2007; Greenwood et al. 2010; Chaumard & Devouard 2016).

Several studies have proposed that CV and CK carbonaceous chondrites originated from the same parent body, with CK chondrites representing thermally equilibrated CV chondrites Greenwood et al. 2003). (Greenwood et al. 2004; The metamorphic progression appears continuous between CV and CK chondrites, with peak metamorphic temperatures ranging from <850 K for CVs, 850–920 K for CK3, and 920–1140 K for CK4–6 (Chaumard & Devouard 2016).

Indeed, ordinary, enstatite, and carbonaceous chondrite groups represent distinct compositional regimes in the solar nebula, spanning from highly reduced (with all Fe present as metal) to fully oxidized (where Fe is entirely incorporated into silicates and oxides), with only rare exceptions deviating from this trend (Righter & Neff 2007). The oxidation conditions of CV and CK chondrites appear continuous or very similar, with the oxidized CV subgroup showing the closest affinity to CK chondrites. The data from the NWA 16813 CK6 chondrite presented in this study further support Righter & Neff (2007)'s interpretation, which contrasts markedly with the previous hypothesis.

2. Material and Methods

The NWA 16813 sample was made into a one-inch epoxy mount. The petrography analysis was carried out using a JEOL JSM-IT500 tungsten filament scanning electron microscope at the State Key Laboratory of Lunar and Planetary Sciences, Macau University of Science and Technology. The microscope is equipped with an Oxford energy dispersive spectrometer (EDS), which was used for both point analysis and mapping analysis.

The major (more than 1.0 wt.%) and minor (less than 1.0 wt.%) element concentrations of olivine, pyroxene, plagioclase, magnetite, ilmenite, and pentlandite were analyzed using a JEOL JXA-iSP100 electron probe microanalyzer (EPMA) also at the State Key Laboratory of Lunar and Planetary Sciences, Macau University of Science and Technology. The conditions for the EPMA analysis were as follows: an acceleration voltage of 15 kV, a probe current of 20 nA, a peak counting time of 30 s, and a background counting time of 15 s. The elemental data were calibrated using a series of natural minerals and synthetic materials. Based on the analysis of internal laboratory standards, the precision for major elements (more than 1.0 wt.%) and minor

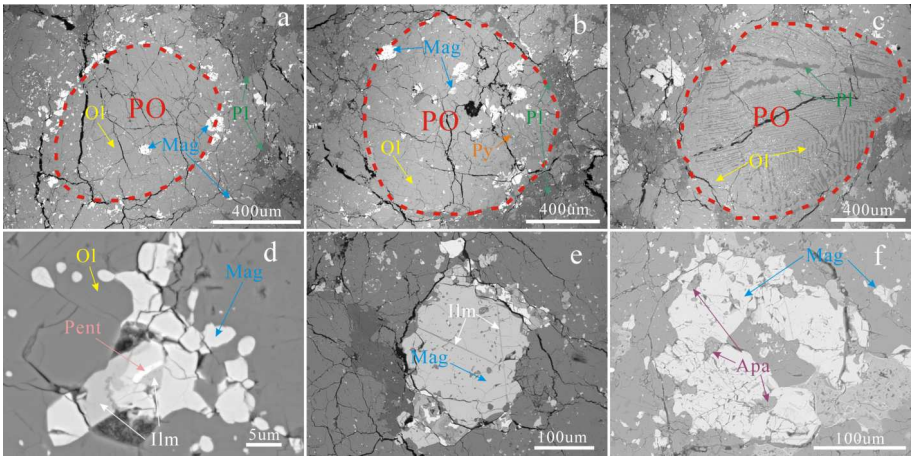

Figure 1. Back scattered electron (BSE) images of the CK chondrite NWA 16813. (a), (b), (c): representative PO chondrules. Magnetite can be found both within the chondrules and at their boundaries; (c): In PO chondrites, the olivine is replaced and filled by plagioclase; (d): the coexisting minerals magnetite, ilmenite and pentlandite; (e): needle-like ilmenite in magnetite is very common; (f): apatite can be found in magnetite. Abbreviations: PO = Porphyritic olivine, Ol = olivine, Pl = plagioclase, Mag = magnetite, Py = pyroxene, Pent = pentlandite, Ilm = ilmenite, Apa = apatite.

elements (less than 1.0 wt.%) is better than 1.5% and 5.0%, respectively.

3. Petrography and Mineralogy

3.1. Petrography

3.1.1. Overall Texture and Modal Abundance

NWA 16813 shows a typical chondritic texture, mainly consisting of chondrules, isolated silicates and opaque minerals set in a fine-grained matrix (Figure 1).

The modal abundances of NWA 16813 were calculated using ImageJ software based on EDS mapping data. The most abundant mineral is olivine at 55 vol.%, followed by plagioclase at 20 vol.%, pyroxene at 13 vol.%, magnetite at 5 vol.%, and sulphides and other phases at 7 vol.%.

Secondary plagioclase is present in both chondrules and matrix, with a grain size ranging from 50 to 600 μm.

3.1.2. Chondrules

The chondrule boundaries in NWA 16813 are diffuse (Figure 1(a)–(c)). Based on EDS mapping data, we identified 20 chondrules with an average diameter of 0.72 mm, consistent with the typical chondrule size (0.8 mm) reported for CK chondrites (Scott & Krot 2003).

Only porphyritic olivine (PO) chondrules were observed. Chondrules consist primarily of olivine, plagioclase, pyroxene, magnetite, ilmenite, pentlandite, and apatite. The olivine and pyroxene grains within the chondrules do not exhibit secondary diffusional zoning. A special chondrule was discovered where the olivine within the chondrule is extensively filled with plagioclase (Figure 1(c)).

3.1.3. Matrix

The matrix of NWA 16813 is composed of fine-grained olivine, plagioclase, opaque minerals (mainly magnetite and rare sulphides), and pyroxene.

3.2. Mineralogy

3.2.1. Olivine

Table 1 presents the EPMA analysis results for olivine. Olivine is most common in chondrules and matrix. The mean Fo value of olivine is 67.36, with a corresponding percent of mean deviation (PMD) of 1.67. The range of Fo values is 64.60–68.64.

3.2.2. Pyroxene

Table 2 presents the EPMA analysis results for pyroxene. Pyroxene is divided into low-Ca (<0.15 atomic Ca/(Ca+Mg +Fe)) and high-Ca pyroxene (or Ca-pyroxene). The mean Fs of low-Ca pyroxene is 30.12, its range is 28.82–32.99, and the PMD is 4.52; the mean Wo of low-Ca pyroxene is 0.79, its range is 0.44–1.91, and the PMD is 60.50. The mean Fs of Ca-pyroxene is 12.18, its range is 10.64–14.08, and the PMD is 11.94; the mean Wo of Ca-pyroxene is 45.14, its range is 41.09–46.72, and the PMD is 6.00.

3.2.3. Plagioclase

Table 3 presents the EPMA analysis results for plagioclase. Plagioclase compositions are heterogeneous, and An value ranges from 18.41 to 46.49.

Table 1
Representative Chemical Compositions (wt.%) of Olivine of CK Chondrite NWA 16813

Point	K_2O	CaO	Al_2O_3	SiO_2	Cr_2O_3	MnO	Na_2O	MgO	TiO_2	FeO	NiO	Total	Fo
Ol1	0.00	0.07	0.02	37.24	0.00	0.25	0.00	33.41	0.00	28.25	0.68	99.92	67.83
Ol2	0.00	0.00	0.02	37.60	0.01	0.25	0.02	32.92	0.00	27.83	0.58	99.23	67.83
Ol3	0.00	0.01	0.02	37.84	0.01	0.24	0.00	33.90	0.02	27.87	0.65	99.55	67.78
Ol4	0.00	0.01	0.02	37.40	0.02	0.24	0.00	32.73	0.03	28.24	0.52	99.19	67.38
Ol5	0.00	0.03	0.02	37.88	0.07	0.24	0.00	33.09	0.00	27.98	0.62	99.90	67.83
Ol6	0.00	0.09	0.02	37.85	0.07	0.24	0.00	31.93	0.00	27.93	1.05	99.24	67.09
Ol7	0.00	0.00	0.02	36.97	0.04	0.27	0.00	32.79	0.00	28.48	0.39	99.04	67.24
Ol8	0.01	0.01	0.02	37.65	0.02	0.24	0.04	33.26	0.00	27.10	0.67	99.22	68.64
Ol9	0.00	0.18	0.02	37.48	0.04	0.46	0.05	30.61	0.03	29.89	0.84	99.65	64.60

Note. Fo = 100 × Mg/(Mg+Fe) in mole.

Table 2
Representative Chemical Compositions (wt.%) of Pyroxene of CK Chondrite NWA 16813

Point	K_2O	CaO	Al_2O_3	SiO_2	Cr_2O_3	MnO	Na_2O	MgO	TiO_2	FeO	NiO	Total	Wo	Fs
Py1	0.00	0.47	0.46	49.20	0.05	0.33	0.02	27.50	0.00	21.42	0.44	99.87	0.84	30.15
Py2	0.02	0.39	0.83	53.11	0.02	0.44	0.02	25.18	0.00	19.31	0.38	99.69	0.78	29.85
Py3	0.03	0.42	0.82	48.72	0.06	0.46	0.07	25.72	0.00	22.84	0.34	99.51	0.78	32.99
Py4	0.02	0.26	0.40	52.70	0.01	0.49	0.03	24.79	0.01	20.00	0.46	99.16	0.52	31.00
Py5	0.00	0.27	0.51	53.40	0.06	0.32	0.01	25.81	0.00	19.02	0.18	99.59	0.53	29.10
Py6	0.01	0.95	1.04	53.04	0.06	0.41	0.09	24.68	0.02	18.74	0.47	99.52	1.91	29.30
Py7	0.00	0.22	1.15	53.26	0.06	0.52	0.02	24.98	0.00	19.01	0.57	99.80	0.44	29.79
Py8	0.00	0.27	0.70	53.70	0.05	0.38	0.00	25.79	0.00	18.75	0.18	99.82	0.52	28.82
Py9*	0.00	22.86	2.93	49.75	0.06	0.10	0.51	14.65	0.20	7.29	0.56	98.95	46.72	11.62
Py10*	0.01	21.92	4.91	48.97	0.03	0.13	0.48	13.30	0.53	8.49	0.41	99.17	46.60	14.08
Py11*	0.00	21.71	2.17	52.27	0.07	0.20	0.41	14.61	0.06	6.41	1.34	99.35	46.16	10.64
Py12*	0.00	19.45	2.20	52.36	0.10	0.23	0.41	15.83	0.08	7.50	1.13	99.28	41.09	12.37

Note. Analysis point name with * meaning high-Ca pyroxene, while others are low-Ca pyroxene.

3.2.4. Magnetite

Magnetite can be found in chondrules, edges of chondrules and matrix (Figure 1(a), (b), (d), (e), (f)). The grain size of magnetite ranges from 5 to 300 μm. Ilmenite exsolution is commonly observed within magnetite grains (Figure 1(d), (e)). Some apatite can also be found in magnetite grains (Figure 1(f)).

Representative EPMA results for magnetite are shown in Table 4. The results indicate that the magnetite in NWA 16813 is chromium-rich magnetite, with a Cr_2O_3 content (wt.%) of 3.48–4.87. The Al_2O_3 content in the magnetite is 0.31–1.91 wt.%, the MgO content is 0.06–0.19 wt.%, and the Fe_2O_3 content is 58.85–63.48 wt.%.

3.2.5. Pentlandite

Pentlandite is the only sulphide found in NWA 16813. The grain size of pentlandite ranges from 5 to 35 μm. Some pentlandites are coexisting with Fe-Ti oxides (Figure 1(d)). Table 5 presents the EPMA analysis results for pentlandite, and the atomic ratio of metal to sulfur in all tested pentlandites is close to 1.1, which is almost identical to the composition of pentlandite ($(Fe, Ni)_9S_8$) and distinctly different from that of Fe-rich monosulphide solid solution (MSS). MSS ($(Fe, Co, Ni)_{1-x}S$) was also reported in CK chondrites (Geiger & Bischoff 1995), and it coexists with pentlandite in the same phase region at around 600°C.

4. Discussion

4.1. Classification Based on Petrographic Characteristics

NWA 16813 has a high abundance of magnetite (approximately 5 vol.%), which falls within the range of magnetite in CK chondrites (1–8 vol.%, with an average of 4 vol.%) (Geiger & Bischoff 1995). No iron-nickel metal was found, consistent with the highly oxidized nature of CK chondrites. The average diameter of identified chondrules is 0.72 mm, which is similar to that of CK4-6 chondrites (0.5–1.1 mm, with an average of 0.6 mm) (Chaumard & Devouard 2016). The proportion of identified chondrules in NWA 16813 (approximately 9 vol.%) is significantly lower than in CK3 and CV3

Table 3
Representative Chemical Compositions (wt.%) of Plagioclase of CK Chondrite NWA 16813

Point	K_2O	CaO	Al_2O_3	SiO_2	Cr_2O_3	MnO	Na_2O	MgO	TiO_2	FeO	NiO	Total	An	Or
Pl1	0.43	8.05	25.83	56.10	0.01	0.00	8.84	0.00	0.00	0.53	0.06	99.84	32.79	2.08
Pl2	0.48	7.70	25.25	57.05	0.00	0.00	8.59	0.18	0.00	0.59	0.00	99.83	32.33	2.39
Pl3	1.28	4.19	22.46	61.79	0.03	0.01	9.43	0.02	0.00	0.59	0.02	99.81	18.41	6.69
Pl4	1.07	6.04	22.78	55.50	0.26	0.01	6.84	0.28	0.09	5.89	0.27	99.03	30.69	6.49
Pl5	4.95	4.00	22.11	61.26	0.05	0.01	6.41	0.05	0.00	0.49	0.10	99.43	18.61	27.45
Pl6	0.19	12.09	29.64	50.01	0.01	0.00	7.57	0.03	0.00	0.43	0.03	99.99	46.49	0.87
Pl7	0.23	10.46	28.28	52.17	0.00	0.00	8.56	0.03	0.00	0.62	0.00	99.85	41.02	1.07
Pl8	0.87	4.12	22.17	62.31	0.02	0.00	8.84	0.00	0.00	0.79	0.02	99.14	19.49	4.92
Pl9	0.32	9.97	27.59	52.25	0.03	0.01	8.70	0.20	0.00	0.57	0.08	99.72	38.22	1.44
Pl10	0.24	11.14	28.85	51.10	0.04	0.02	7.24	0.02	0.00	0.87	0.06	99.57	45.43	1.17

Table 4
Representative Chemical Compositions (wt.%) of Magnetite and Coexisting Ilmenite of CK Chondrite NWA 16813

Point	CaO	FeO^*	Cr_2O_3	Al_2O_3	SiO_2	TiO_2	NiO	ZnO	ZrO_2	MnO	V_2O_3	MgO	$Fe_2O_3{}^*$	Total
Mag1	0.00	31.73	3.60	0.37	0.05	0.52	0.17	0.06	0.00	0.07	0.13	0.10	61.67	98.46
ilm1	0.03	40.93	2.36	8.38	0.15	43.16	0.07	0.24	0.00	0.74	0.35	2.58	0.00	98.97
Mag2	0.06	30.24	4.71	1.91	0.02	0.32	0.21	0.00	0.00	0.06	0.15	0.19	60.55	98.43
ilm2	0.13	40.36	4.16	9.94	0.05	40.31	0.04	0.46	0.08	0.63	0.34	2.78	0.00	99.27
Mag3	0.19	31.36	4.87	1.73	0.03	0.54	0.27	0.03	0.08	0.04	0.11	0.17	59.68	99.09
ilm3	0.33	44.68	1.64	1.17	0.09	48.67	0.07	0.00	0.01	0.67	0.38	1.58	0.00	99.28
Mag4	0.00	30.98	4.45	0.87	0.02	0.31	0.22	0.00	0.05	0.06	0.13	0.13	61.74	98.98
ilm4	0.17	41.35	3.76	7.91	0.15	42.19	0.13	0.25	0.05	0.71	0.37	2.40	0.00	99.42
Mag5	0.00	31.18	4.34	0.73	0.01	0.23	0.20	0.00	0.02	0.03	0.13	0.13	61.44	98.46
ilm5	0.13	41.04	3.07	7.24	0.03	43.87	0.00	0.36	0.00	0.68	0.35	2.64	0.00	99.42
Mag6	0.01	31.54	3.95	0.55	0.01	0.31	0.18	0.00	0.00	0.04	0.13	0.09	61.39	98.20
ilm6	0.14	40.74	4.75	9.00	0.04	40.82	0.07	0.31	0.03	0.59	0.34	2.36	0.00	99.19
Mag7	0.00	31.30	4.10	0.76	0.02	0.42	0.17	0.00	0.02	0.04	0.13	0.10	61.13	98.17
ilm7	0.01	43.30	2.21	4.03	0.06	46.96	0.03	0.14	0.02	0.67	0.36	2.04	0.00	99.83
Mag8	0.04	31.67	4.52	0.94	0.02	1.84	0.11	0.00	0.01	0.08	0.15	0.13	58.85	98.36
ilm8	0.10	44.35	1.45	1.20	0.01	49.79	0.03	0.00	0.00	0.80	0.38	1.55	0.00	99.66
Mag9	0.01	30.60	4.75	1.34	0.02	0.26	0.23	0.00	0.00	0.03	0.13	0.18	60.71	98.25
ilm9	0.09	43.31	4.36	3.70	0.11	44.40	0.07	0.08	0.02	0.71	0.36	1.81	0.00	99.01
Mag10	0.00	31.66	3.77	0.71	0.05	0.19	0.19	0.04	0.00	0.02	0.11	0.14	61.44	98.31
ilm10	0.05	40.60	3.09	7.62	0.05	42.60	0.09	0.27	0.06	0.62	0.36	2.70	0.00	98.11
Mag11	0.00	30.94	4.25	0.87	0.00	0.28	0.18	0.03	0.00	0.05	0.14	0.07	62.43	99.24
ilm11	0.09	42.27	3.21	7.73	0.03	42.27	0.04	0.00	0.08	0.64	0.32	2.78	0.00	99.43
Mag12	0.00	30.85	4.31	0.78	0.00	0.21	0.17	0.02	0.00	0.06	0.13	0.06	62.73	99.31
ilm12	0.34	42.93	3.21	4.57	0.04	44.87	0.08	0.00	0.11	0.68	0.25	2.25	0.00	99.31
Mag13	0.00	30.56	3.78	0.31	0.03	0.16	0.18	0.00	0.05	0.01	0.10	0.10	63.48	98.75
ilm13	0.08	41.79	4.19	9.72	0.07	38.43	0.06	0.01	0.06	0.66	0.34	2.68	0.00	98.09
Mag14	0.07	30.33	3.48	0.31	0.11	0.14	0.23	0.00	0.00	0.03	0.13	0.08	63.23	98.15
ilm14	0.12	38.96	3.63	8.70	5.08	34.57	0.19	0.00	0.11	0.66	0.27	7.98	0.00	100.28

Note. The contents of FeO^* and Fe_2O_3 were calculated from stoichiometry (Droop 1987).

chondrites (CV3: 18.5–55.7 vol.%; CK3: 17.1–25.7 vol.%). The size range of secondary plagioclase grains (diameter ranges from 50 to 600 μm) is consistent with that of CK6 chondrites (CK5: $4\,\mu\text{m} < D < 50\,\mu\text{m}$; CK6: $D > 50\,\mu\text{m}$. D = diameter) (Kallemeyn et al. 1991). Based on the above petrographic characteristics, NWA 16813 is classified as a CK6 carbonaceous chondrite.

4.2. Classification Based on Mineralogical Characteristics

The main petrographic classification criteria for the CK group can be summarized by mineralogy characteristics (Geiger & Bischoff 1991). (1) Presence of equilibrated olivines with mean Fa contents between 28 and 33 mol%, 0.5 wt.% NiO, <0.1 wt.% CaO. (2) Occurrence of two

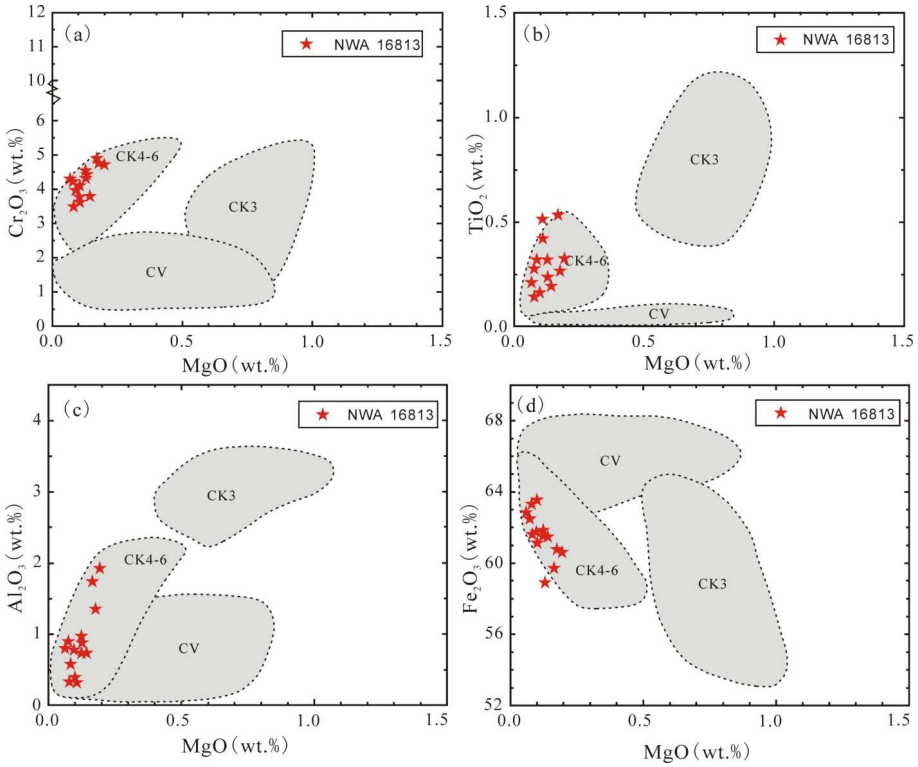

Figure 2. Chemical compositions of magnetite in NWA 16813. Data for CK3 (Dunn et al. 2016), CK4-6 (Geiger & Bischoff 1995; Greenwood et al. 2010; Rubin 1993; Chaumard et al. 2014; Davidson et al. 2014) and CV (Haggerty & Mcmahon 1979; Rubin 1991; Murakami & Ikeda 1994; Greenwood et al. 2010) are plotted for comparison. Fe_2O_3 contents are stoichiometric results (Droop 1987).

Table 5
Representative Chemical Compositions (wt.%) of Plagioclase of CK Chondrite NWA 16813

Point	Cu	Ni	S	Fe	Co	O	Total	Metal/S(Atomic Ratio)
S1	0.03	35.82	32.94	28.35	1.28	0.36	98.77	1.09
S2	0.03	37.36	32.81	27.13	1.04	0.60	98.95	1.10
S3	0.03	39.46	33.01	26.34	0.67	0.44	99.96	1.11
S4	0.02	38.67	30.56	24.11	0.90	3.54	97.80	1.14
S5	0.05	40.57	32.45	24.66	0.63	0.75	99.11	1.12
S6	0.04	35.93	32.92	29.16	0.78	0.46	99.29	1.11
S7	0.03	36.24	33.06	29.23	1.01	0.54	100.11	1.11
S8	0.05	38.19	32.49	26.99	0.92	0.48	99.11	1.12
S9	0.00	35.84	32.93	28.98	1.07	0.86	99.67	1.10
S10	0.00	35.59	32.84	28.87	1.07	0.58	98.95	1.10
S11	0.00	36.28	33.23	29.42	0.76	0.53	100.21	1.10
S12	0.08	36.68	32.77	28.47	0.80	0.49	99.29	1.11
S13	0.09	40.21	32.76	25.19	0.61	0.57	99.43	1.11
S14	0.05	36.30	32.94	28.93	0.98	0.48	99.67	1.11
S15	0.02	36.76	32.44	28.68	0.91	0.76	99.57	1.13
S16	0.04	36.07	32.87	28.97	1.35	0.51	99.81	1.11
S17	0.00	36.15	31.90	28.40	1.24	0.75	98.44	1.13

different pyroxenes: low-Ca pyroxene (Fs_{24-28}) and augitic pyroxenes (Fs_{8-12}). (3) Presence of heterogeneous plagioclase varying compositionally between An_{20} and An_{75}. For some CK chondrites bimodal distributions were found (Keller 1993; Noguchi 1993). (4) Occurrence of several opaque phases: (a) abundant magnetite (commonly containing exsolution lamellae of spinel and ilmenite), (b) various Fe- and Ni-rich sulphides (including pentlandite, pyrite, pyrrhote and Fe-rich MSS), and (c) sulphides, tellurides and arsenides rich in refractory siderophile elements (Pt, Os, Ir, Ru), and in Au and Ag.

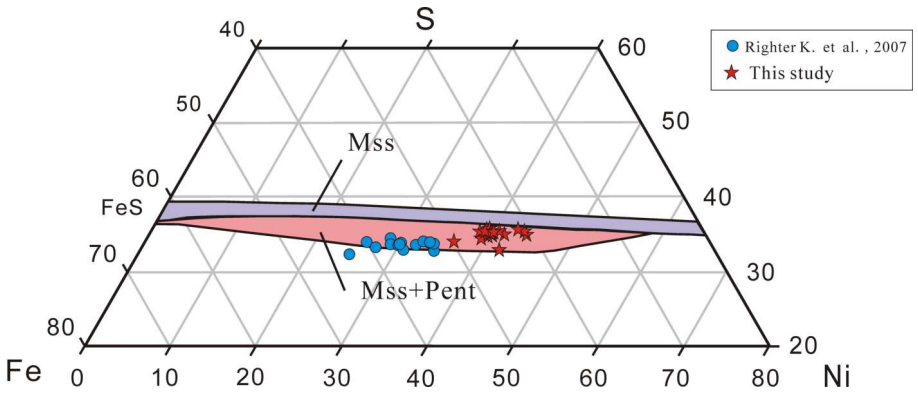

Figure 3. Phase diagram for the Fe-Ni-S system at 600°C (from Craig 1973). The composition of pentlandite is from CK chondrites in this study and from Righter & Neff (2007) for comparison. MSS = Fe-rich monosulphide solid solution, $(Fe, Co, Ni)_{1-x}S$; Pent = pentlandite, $(Fe, Ni)_9S_8$.

Table 6
The Temperature (°C) and Oxygen Fugacity (fO_2) Calculated Based on Magnetite and Ilmenite Pairs in NWA 16813

No.	T1	T2	T3	T4	$T_{average}$	F1	F2	F3	F4	$F_{average}$	ΔFMQ
Mag1	665.00	604.20	587.16	608.53	616.22	−13.82	−16.71	−17.90	−16.82	−16.31	4.02
Mag2	645.92	603.16	586.99	613.93	612.50	−13.69	−15.71	−16.90	−15.61	−15.48	4.85
Mag3	598.33	552.16	546.54	564.11	565.28	−17.32	−20.24	−20.72	−19.83	−19.53	0.80
Mag4	638.26	586.84	573.97	596.28	598.84	−14.00	−16.54	−17.59	−16.47	−16.15	4.17
Mag5	615.92	559.79	544.77	568.06	572.13	−14.49	−17.68	−18.86	−17.56	−17.14	3.18
Mag6	640.95	593.93	578.06	602.08	603.76	−13.81	−16.20	−17.33	−16.11	−15.86	4.46
Mag7	622.35	560.93	550.59	565.59	574.87	−15.41	−19.02	−19.84	−19.08	−18.34	1.99
Mag8	637.59	573.79	566.45	579.54	589.34	−17.55	−21.37	−21.88	−21.24	−20.51	−0.19
Mag9	615.01	566.07	558.04	572.53	577.91	−14.87	−17.60	−18.27	−17.61	−17.09	3.24
Mag10	621.68	560.80	544.81	566.51	573.45	−14.30	−17.20	−18.40	−17.20	−16.78	3.55
Mag11	629.03	593.12	580.18	599.29	600.40	−14.09	−15.95	−16.96	−16.05	−15.76	4.56
Mag12	599.76	550.39	545.07	563.49	564.68	−15.04	−17.84	−18.61	−17.61	−17.28	3.05
Mag13	619.38	588.10	572.45	589.78	592.43	−13.95	−15.18	−16.19	−15.32	−15.16	5.17
Mag14	638.63	597.83	596.75	601.33	608.63	−13.70	−14.22	−14.52	−14.41	−14.21	6.11

Note. T1, T2, T3 and T4 are temperature data, and F1, F2, F3 and F4 are oxygen fugacity data. $T_{average}$ is the average value of T1, T2, T3 and T4; $F_{average}$ is the average value of F1, F2, F3 and F4. The T1 and F1 data are based on the method of Carmichael (1966), the T2 and F2 data are based on the method of Anderson (1968), the T3 and F3 data are based on the method of Lindsley & Spencer (1982), and the T4 and F4 data are based on the method of Stormer (1983).

The average Fa value of olivine in NWA 16813 is 32.64, falling between 28 and 33 mol%; the average NiO content of olivine is 0.67 wt.%, close to 0.5 wt.%; and the CaO content is 0.04 wt.%, which is far less than 0.1 wt.%.

The average Fs value of low-Ca pyroxene in NWA 16813 is 30.12, close to the range of 24–28. The average Fs value of Ca-pyroxene is 12.18, very close to the ranges of augitic pyroxene ($Fs_{8\text{-}12}$) reported in previous studies.

The range of An value is from 18.41 to 46.49, indicating a wide variation. Almost all An values of the plagioclase grains fall within the An_{20}–An_{75} range.

Magnetite in carbonaceous chondrites is generally considered to be a product of low-temperature aqueous alteration of metal (Choi et al. 2000). Since magnetite is relatively resistant to terrestrial weathering, it can be assumed that terrestrial weathering has little effect on its composition. However, the chemical composition of magnetite may have been altered by later thermal metamorphism on the parent body. Therefore, the chemical composition of magnetite can be used to effectively distinguish between CV, CK3, and CK4-6 chondrites (Dunn et al. 2016).

The major elemental chemical composition (Fe_2O_3) and minor elemental chemical composition (MgO, Cr_2O_3, TiO_2, and Al_2O_3) of magnetite in NWA 16813 are compared with those reported in previous studies for CK3 (Dunn et al. 2016), CK4-6 (Geiger & Bischoff 1995; Greenwood et al. 2010; Rubin 1993; Chaumard et al. 2014; Davidson et al. 2014), and CV (Haggerty & Mcmahon 1979; Rubin 1991; Murakami & Ikeda 1994; Greenwood et al. 2010) chondrites, as shown in Figure 2. The results indicate that, except for a titanium-poor magnetite and a low-Fe_2O_3 magnetite, the chemical compositions of most magnetites in NWA 16813 fall within the range of CK4-6 chondrites.

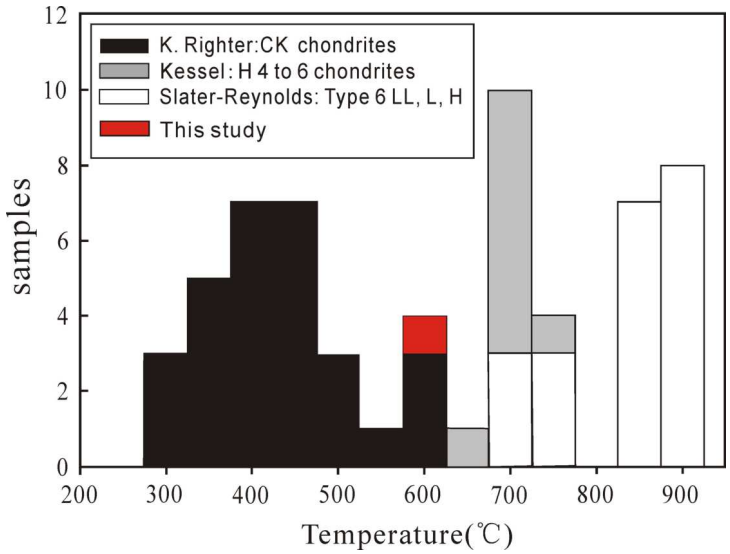

Figure 4. Histogram of temperature calculated for CK chondrite NWA 16813 in this study, compared to those calculated for equilibrated CK chondrites and ordinary chondrites from the studies of Kessel et al. (2004) and Slater-Reynolds & Mcsween (2005).

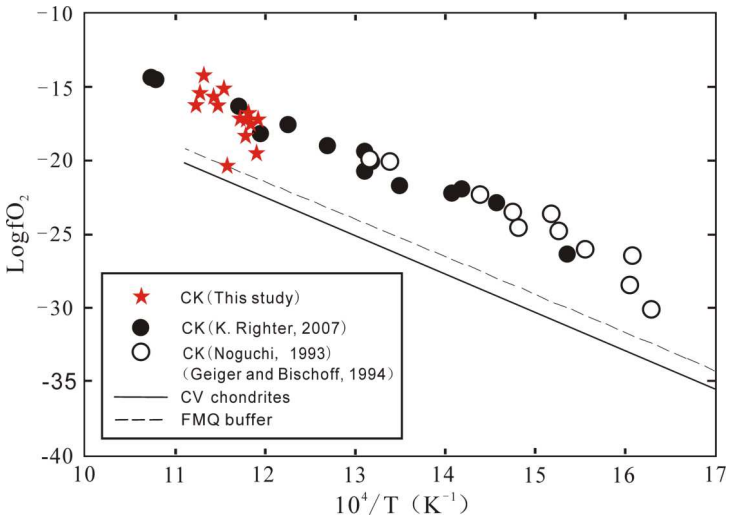

Figure 5. Log fO_2 vs. Inverse temperature ($104/T(K^{-1})$) calculated using ilmenite-magnetite pairs in CK chondrites. Closed circles are CK data from Righter & Neff (2007), and open circles are CK data from Noguchi (1993) and Geiger & Bischoff (1995). Log fO_2 is a function of temperature for metal-magnetite pairs in CV chondrites (Righter & Neff 2007).

4.3. Temperature and Oxygen Fugacity

4.3.1. Temperature

Iron-titanium oxides in igneous rocks or metamorphic rocks are widely used to calculate and constrain the physicochemical conditions in the process of magma crystallization or metamorphism, particularly for determining the equilibrium temperature and oxygen fugacity. A series of iron-titanium oxide thermometers and oxygen fugacity meters have been established (Yavuz 2021). WinMlgob is a software tool that compiles and directly executes the calculation methods of iron-titanium oxide thermometers and oxygen fugacity meters (Yavuz 2021). In this paper, WinMlgob was used to perform the temperature and oxygen fugacity calculations. The calculated methods of Carmichael (1966), Anderson (1968), Lindsley & Spencer (1982), Stormer (1983) were selected, and the calculations were performed based on the calibrations of Andersen & Lindsley (1985).

The temperature and oxygen fugacities of NWA 16813 were calculated based on 14 magnetite and ilmenite pairs, and are shown in Table 6. The calculated temperature range is

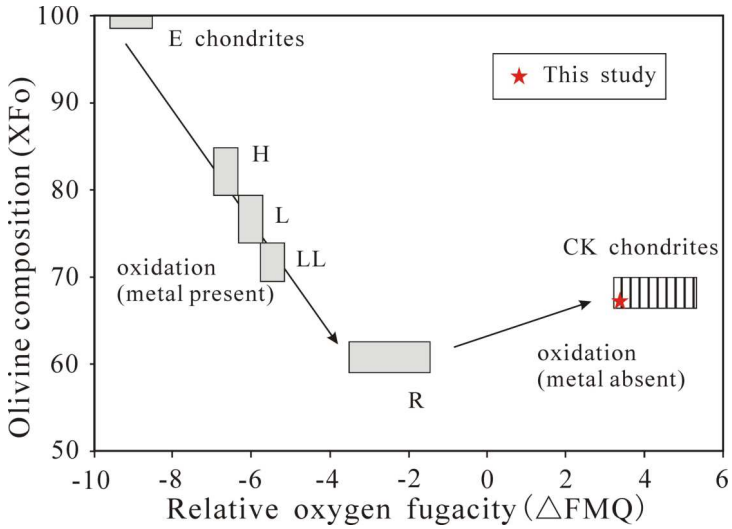

Figure 6. A plot of relative oxygen fugacity vs. olivine composition (XFo) for a number of equilibrated chondrites (enstatite, ordinary, R, and CK chondrites). The trend from reduced E to oxidized R chondrites can be explained by progressive oxidation of FeNi metal. CK chondrites fall off of this trend at more forsteritic olivine compositions; this can be explained by oxidation in the absence of metal (Righter & Neff 2007). Fields for E, H, L, LL, and R chondrite groups are from data summarized in Righter & Neff (2007).

564.68–616.22°C, and average temperature is 587.32°C, which is within the range of 300–658°C of CKs calculated by Righter & Neff (2007). This lower temperature is further supported by the presence of pentlandite (Figure 1(d); Figure 3), which is not stable at temperatures greater than 883 K (610°C), and is distinguished from MSS based on the atomic ratio of metal to sulfur (S). The phase diagram of pentlandite in this study is more concentrated than that of Righter & Neff (2007).

Re-equilibrium temperatures calculated for the CK6 chondrite NWA 16813 in this study are compared to temperatures of CK and R chondrites calculated by Righter & Neff (2007) and ordinary chondrites (Figure 4; Kessel et al. 2004; Slater-Reynolds & Mcsween 2005). The temperatures calculated for NWA 16813 in this study rank among the highest temperatures calculated by Righter & Neff (2007), and are much lower than those calculated for type 6 ordinary chondrites by Kessel et al. (2004) based on olivine-spinel equilibrium, and Slater-Reynolds & Mcsween (2005) based on two cases of pyroxene thermometry. Although some of this discrepancy may be attributed to differences in thermometers used in the various studies, it may also indicate that CKs record lower metamorphic re-equilibration temperatures in the type 6 oxidized chondrites. Besides, the re-equilibration temperature of NWA 16813 is close to the lower limit of the peak metamorphic temperature 920–1140 K (645°C–865.85°C) calculated by Chaumard & Devouard (2016).

4.3.2. Oxygen Fugacity

Petrologic evidence for an oxidized formation of CK chondrites includes the absence of Fe-Ni metal and the abundance of magnetite (Geiger & Bischoff 1995). The CV chondrites contain Fe-Ni metal in the reduced and oxidized subgroups (Krot et al. 2004), and even the oxidized CVs are more reduced than the CK chondrites since they contain metal.

Oxygen fugacities, recorded by coexisting magnetite-ilmenite pairs in the CK chondrites studied here, range from log $fO_2 = -20.51$ (589.34°C) to -14.21 (608.63°C). The CK temperature and oxygen fugacity plot forms a linear trend, shown in Figure 5, suggesting they equilibrated across a small range of temperature, but parallel to an oxygen buffer.

4.4. The Relationship Between CV and CK

The CV and CK carbonaceous chondrite groups have been compared to each other often because of petrographic similarities, and overlapping oxygen isotopic ratios, similar cosmic-ray exposure age distributions and consistent reflectance spectral characteristics. Some have suggested the two groups of carbonaceous chondrites formed from the same parent body and CKs are equilibrated CVs (Greenwood et al. 2003; Greenwood et al. 2004). The oxidized CVs have been most closely related to CKs, the peak metamorphic temperatures of CV and CK3, CK4-6 are continual, and all these conditions constraining the formation of meteorite seem to support the above viewpoint. However, the oxygen fugacity reported in this study does not support it.

Oxygen fugacities calculated for CK chondrites in this study and from Righter & Neff (2007), Noguchi (1993) and Geiger & Bischoff (1995) are always higher than those for CVs, as much as 4 or 4 log fO_2 units higher. This suggests that if CKs were derived from CVs, the metamorphic conditions or fluids were very oxidizing.

Besides, relative oxygen fugacity and olivine composition (Fo) show that CKs are depleted in metal compared to CVs, not just because CK chondrites are more oxidized than CV chondrites (Figure 6).

5. The Future Plan

CK chondrites are the most oxidized chondrites, and the mechanism behind their oxidation has not yet been studied in detail, warranting further investigation.

Acknowledgments

This work is supported by the Science and Technology Development Fund of Macau (FDCT) (grant 002/2024/SKL). The author is very grateful to Prof. Weibiao Hsu at the Purple Mountain Observatory, Chinese Academy of Sciences for providing many important suggestions for revisions before submitting the manuscript, and I also thank Mr. Fujun Ren for providing the meteorite sample needed for this study. The reviewer promptly reviewed this paper and provided some valuable comments, for which I also extend my gratitude. Finally, I would like to express my sincere gratitude to the Editor, James Wicker, who did a great deal of meticulous editing work on this article, significantly enhancing its readability and accuracy.

References

Anderson, A. T. 1968, JG, 76, 528
Andersen, D. J., & Lindsley, D.H. 1985, Eos, TAGU, 66, 416
Carmichael, I. S. E. 1966, CoMP, 14, 36
Chaumard, N., & Devouard, B. 2016, M&PS, 51, 547
Chaumard, N., Devouard, B., Bouvier, A., & Wadhwa, M. 2014, M&PS, 49, 419
Choi, B. G., Krot, A. N., & Wasson, J. T. 2000, M&PS, 35, 1239
Craig, J. R. 1973, AmJS, 273, 496
Davidson, J., Krot, A. N., Nagashima, K., Hellebrand, E., & Lauretta, D. S. 2014, M&PS, 49, 1456
Droop, G. T. R. 1987, MinM, 51, 431
Dunn, T. L., Gross, J., Ivanova, M. A., Runyon, S. E., & Bruck, A. M. 2016, M&PS, 51, 1701
Geiger, T., & Bischoff, A. 1991, Metic, 26, 337
Geiger, T., & Bischoff, A. 1995, P&SS, 43, 485
Greenwood, R. C., Franchi, I. A., Kearsley, A. T., & Alard, O. 2004, LPS, 1, 1664
Greenwood, R. C., Franchi, I. A., Kearsley, A. T., & Alard, O. 2010, GeCoA, 74, 1684
Greenwood, R. C., Kearsley, A. T., & Franchi, I. A. 2003, AMSM, 1, 5179
Haggerty, S. E., & Mcmahon, B. M. 1979, LPSC, 10, 482
Kallemeyn, G. W., Rubin, A. E., & Wasson, I. T. 1991, GeCoA, 55, 881
Keller, L. P. 1993, LPSC, 1, 783
Kessel, R., Beckett, J. R., Huss, G. R., & Stolper, E. M. 2004, M&PS, 39, 1287
Krot, A. N., Petaev, M. I., & Bland, P. A. 2004, AMR, 17, 153
Lindsley, D. H., & Spencer, K. J. 1982, Eos, TAGU, 63, 471
Murakami, T., & Ikeda, Y. 1994, M&PS, 29, 397
Noguchi, T. 1993, NIPR, 6, 204
Righter, K., & Neff, K. E. 2007, PolSc, 1, 25
Rubin, A. E. 1991, AmMin, 76, 1356
Rubin, A. E. 1993, Metic, 28, 130
Scott, E. R. D., & Krot, A. N. 2003, in Treatise on Geochemistry, ed. D. H. Heinrich & K. T. Karl (Amsterdam: Elsevier)
Slater-Reynolds, V., & Mcsween, H. Y., Jr. 2005, M&PS, 40, 745
Stormer, J. C., Jr. 1983, AmMin, 68, 586
Yavuz, F. 2021, JG, 66, 51